Truncated Hemoglobin from the Cyanobacterium *Synechococcus* sp. PCC 7002: Evidence for Hexacoordination and Covalent Adduct Formation in the Ferric Recombinant Protein[†,‡]

Nancy L. Scott,[§] Christopher J. Falzone,[§] David A. Vuletich,[§] Jindong Zhao,[||] Donald A. Bryant,[⊥] and Juliette T. J. Lecomte*[,§]

Department of Chemistry and Center for Biomolecular Structure and Function and Department of Biochemistry and Molecular Biology, The Pennsylvania State University, University Park, Pennsylvania 16802, and Department of Plant Molecular Biology, College of Life Sciences, Beijing University, Beijing, China

Received January 31, 2002; Revised Manuscript Received March 15, 2002

ABSTRACT: The *glbN* gene for the hemoglobin of *Synechoccocus* sp. PCC 7002, a cyanobacterium incapable of nitrogen fixation, was cloned and overexpressed in *Escherichia coli*. The 123-residue protein was purified from inclusion bodies and reconstituted with iron protoporphyrin IX to obtain the ferric form of the holoprotein. Mass spectrometric analysis confirmed the identity of the polypeptide. NMR and optical data demonstrated that the protein so prepared contained a hexacoordinate heme group, as observed in the related globin from *Synechocystis* sp. PCC 6803 [Scott, N. L., and Lecomte, J. T. J. (2000) *Protein Sci. 9*, 587−597]. The data were consistent with a similar bis-histidine coordination scheme involving His46 (E10) on the distal side and His70 (F8) on the proximal side. Several aromatic residues were identified in the vicinity of the heme and were used to establish the orientation of the prosthetic group in the polypeptide matrix. In this protein, as in that from *Synechocystis* sp. PCC 6803, there was a marked preference for the heme orientation in which pyrroles C and D contact the C−E corner of the protein. Both hemoglobins were found capable of forming a product in which the heme is cross-linked to the polypeptide through modification of a vinyl group.

Certain cyanobacteria of the genera *Nostoc* and *Synechocystis* contain a gene, *glbN*, that encodes a hemoglobin of approximately 120 residues (*1*−*3*). These cyanobacterial proteins belong to the truncated hemoglobin family (trHb),[1] a distinct phylogenetic group sharing less than 15% sequence similarity with other nonvertebrate and vertebrate globins (*4*). The best-studied member of the trHb family with respect to physiological properties is the hemoglobin from the nitrogen-fixing cyanobacterium *Nostoc commune* (GlbN). In this organism, GlbN is produced with proteins of the nitrogenase complex; it is a peripheral membrane protein that accumulates on the cytosolic side of the cell membrane in both the heterocysts and vegetative cells (*3*). In vitro studies demonstrate that *N. commune* GlbN binds oxygen with high affinity (*5*); its role may be to scavenge oxygen and deliver it to a terminal oxidase (*3*).

Among the 30 strains of filamentous cyanobacteria capable of aerobic N_2 fixation that were screened for the presence of *glbN* in an early study (*3*), fewer than half contained candidate *glbN* genes, demonstrating that GlbN is not essential to nitrogen fixation. No *glbN* gene was found in *Nostoc* sp. PCC 7120 (*Anabaena* sp. PCC 7120), an observation now confirmed with the complete sequencing of the *Anabaena* sp. PCC 7120 genome (*6*). According to recent microbial genome information (*7*), the *glbN* gene is also identified in *Nostoc punctiforme* and in *Chloroflexus aurantiacus*, a filamentous anoxygenic phototroph exhibiting characteristics of both the green sulfur bacteria and the purple bacteria. In contrast, the *glbN* gene appears to be absent from *Prochlorococcus marinus* strains MED4 and MIT9313 and from marine *Synechococcus* sp. WH8102. At this time, the distribution of GlbN-like proteins does not correlate with any obvious physiological or metabolic properties.

The structures of three trHb's, from *Paramecium caudatum*, *Chlamydomonas eugametos*, and *Mycobacterium tuberculosis*, have been solved by X-ray methods (*8*, *9*). In

[†] Supported by National Science Foundation Grants MCB-0091182 (J.T.J.L.) and MCB-0077586 (D.A.B.), USPHS Grant GM-31625 (D.A.B.), and State Key Project of China (G19980101) (J.Z.).

[‡] The DNA sequence was deposited with GenBank (accession number AF475938).

* Corresponding author. Phone: (814) 863-1153. Fax: (814) 863-8403. E-mail: jtl1@psu.edu.

[§] Department of Chemistry, The Pennsylvania State University.

[||] Department of Plant Molecular Biology, Beijing University.

[⊥] Department of Biochemistry and Molecular Biology, The Pennsylvania State University.

[1] Abbreviations: 1D, one-dimensional; 2D, two-dimensional; 2QF-COSY, double-quantum-filtered correlated spectroscopy; dd, distilled deionized; DSS, 2,2-dimethyl-2-silapentane-5-sulfonate; EDTA, ethylenediaminetetraacetic acid; GlbN, cyanoglobin; Hb, hemoglobin; NOE, nuclear Overhauser effect; NOESY, two-dimensional nuclear Overhauser effect spectroscopy; PCR, polymerase chain reaction; rHb, recombinant hemoglobin; rHb-R, recombinant hemoglobin with heme added via a reconstitution protocol; rHb-A, recombinant hemoglobin with covalently attached heme; S6803, *Synechocystis* sp. PCC 6803; S7002, *Synechococcus* sp. PCC 7002; TOCSY, totally correlated two-dimensional spectroscopy; TPPI, time-proportional phase incrementation; trHb, truncated hemoglobin; Tris, tris(hydroxymethyl)aminomethane; WATERGATE, water suppression by gradient-tailored excitation; WEFT, water elimination Fourier transform.

10.1021/bi025609m CCC: $22.00
Published on Web 05/09/2002

each of these structures, the iron ion is coordinated by the proximal histidine and an exogenous sixth ligand. The trHb fold exhibited by these proteins contains unique cavities and tunnels presumably allowing oxygen and other small ligands to access the distal side of the heme group (*4*, *9*). In addition to these static structural features, unusual ligand-dependent conformational changes have been observed in *P. caudatum* Hb, in which they appear to accelerate the ligand dissociation rate (*10*). The number of deletions, insertions, and substitutions in cyanobacterial Hbs compared to other trHbs is large, and predictions based on the available X-ray structures may not be reliable for purposes of predicting chemical properties. The suggestion that trHbs may play catalytic roles (*4*) also warrants a thorough investigation of the range of chemical tasks these proteins can perform.

The truncated hemoglobin from nitrogen-fixation-negative *Synechocystis* sp. PCC 6803 binds oxygen tightly (*11*, *12*), but unlike in *N. commune*, the location of the *glbN* gene within the genome and biochemical analyses have so far provided no hints for its use(s) in the cell. In vivo information on the temporal and spatial distribution of the protein is also lacking. To investigate the relationship between structure and reactivity in a cyanobacterial globin, an NMR study of the recombinant protein from *Synechocystis* sp. PCC 6803 (S6803 rHb-R) was initiated (*13*). This globin has spectroscopic signatures resembling those of cytochrome b_5, and analysis of NMR data identified His46 (residue E10 in the vertebrate globin helix nomenclature) and His70 (proximal, residue F8) as the axial ligands to the ferric heme (*14*). *N. commune* GlbN also contains histidines at positions E10 and F8; it is capable of endogenous hexacoordination under some conditions (*5*, *15*), although the identity of the sixth ligand has not been confirmed. To gain insight into the factors controlling stable bis-histidine hexacoordination, *Synechococcus* sp. PCC 7002 (S7002) was considered as a novel source of cyanobacterial protein. Ongoing systematic genome sequencing has revealed a copy of a *glbN* gene in this euryhaline (brackish water) organism. The primary structure of the protein product is presented in Figure 1, aligned against the *Synechocystis* sp. PCC 6803 and the *N. commune* sequences with BLAST (*16*). The axial histidines of S6803 Hb are conserved in S7002 Hb, and in the present report, it is shown that they also serve as axial ligands to the iron. A novel observation is that this protein forms a covalent adduct to one of the vinyl side chains of the heme.

MATERIALS AND METHODS

Materials. Unless otherwise indicated in the text, chemicals were purchased from Sigma Chemical Co., St. Louis, MO, and enzymes from Promega Corp., Madison, WI.

Cloning, Expression, and Purification of S7002 Hb. The putative hemoglobin gene of *Synechococcus* sp. PCC 7002 was amplified by PCR from a cDNA cosmid. The primers (Integrated DNA Technologies, Coralville, IA) were designed to incorporate 5′-*Nde*I and 3′-*Bam*HI restriction enzyme recognition sites to allow cloning of the gene into a T7 polymerase-controlled expression vector. Following enzymatic digestion, purification, and ligation of the PCR product into the doubly digested pET3c vector (Novagen, Inc., Madison, WI), the resulting plasmid was transformed into, replicated by, and purified (Qiaprep Spin Miniprep Kit, Qiagen, Valencia, CA) from *E. coli* DH5α. The cells were made competent prior to transformation by the modified Simanis method reported for *E. coli* BL21(DE3) (*13*), except rubidium was employed as the monovalent cation in transformation buffers as per the original reference (*17*). Restriction enzyme digestion and DNA sequencing verified the presence of the correct insert in the molecular construct.

The plasmid was transformed into the competent expression host strain *E. coli* BL21(DE3), also prepared by the above method. Freshly transformed cells were seeded into 2 × 25 mL of Luria−Bertani broth [1% (w/v) tryptone, 0.5% (w/v) yeast extract (Difco Laboratories, Detroit, MI), and 1% (w/v) NaCl] supplemented with ampicillin (Kodak, Rochester, NY) to 50 μg/mL (LB/Amp) in 125 mL baffled flasks and shaken at 250 rpm, 37 °C, for approximately 12 h. Optimal expression of the gene did not require induction by IPTG and was continued by transferring 10 mL starter growth to each of four 500 mL volumes of LB/Amp in 2 L baffled flasks and culturing as above for an additional 13 h.

The method generated apoprotein partitioned entirely to inclusion bodies, which was purified using a scheme similar to that used for apo S6803 rHb (*14*) with the following modifications: cell pellets were washed with 50 mM Tris, 1 mM EDTA, pH 8.0, before freezing, rounds of sonication were increased to four, and inclusion body washes were doubled in volume. The elution profile from the Sephadex G-50 Fine sizing column as monitored by UV spectroscopy was similar to that of apo S6803 Hb, and fractions constituting the body of the S7002 rHb peak were pooled, concentrated, and reconstituted with an excess of bovine hemin chloride (50 mg/mL in 0.1 M NaOH) to obtain the holoprotein, S7002 rHb-R. S7002 rHb-R was purified in a final step of DEAE anion-exchange chromatography as detailed previously (*14*). Protein was concentrated and exchanged into 20 mM Na_2H/NaH_2 phosphate, pH 7.5, in an Amicon (Danvers, MA) model 8MC Micro-Ultrafiltration System equipped with a 3000 MW cutoff regenerated cellulose membrane (Millipore, Bedford, MA). This process produced approximately 40 mg of pure holoprotein per liter of culture.

Samples of S6803 rHb-R used for comparison were prepared as previously reported (*14*).

Reduction and Carbon Monoxide Binding. A buffered protein solution registering 0.4−0.6 absorbance unit in the Soret region was reduced by adding a small amount of solid sodium dithionite and mixing end-over-end in a sealed cuvette. To bind ligand, pure carbon monoxide gas was gently bubbled through the solution for approximately 45 s. Absorbance was measured at 1-nm intervals over the range of 250−700 nm. Solution pH was monitored throughout each procedure and remained within 0.5 unit.

Hemochromogen Assay. The millimolar extinction coefficients of ferric S7002 Hb were determined with the hemochromogen method of de Duve (*18*). Hemoglobin concentrations reported in this work are expressed on a heme basis.

Mass Spectrometry. Mass spectrometric data were collected at the Penn State Intercollegiate Center for Mass Spectrometry on a sample of purified ferric S7002 rHb-R. Tryptic digestion was performed in 50 mM ammonium bicarbonate (pH 8) at a trypsin:protein ratio of approximately 1:50. Incubations were carried out at 37 °C for 24 h to 2 weeks. Intact proteins and protein digests were separated

```
                aaaAAAAaa BBBBBBBBBBBBBBBBB  ccCCC  eeeEEEEEEEEEEEEEE

                        1         2         3         4         5         6
                1       0         0         0         0         0         0
Syn 7002        MASLYEKLGGAAAVDLAVEKFYGKVLADERVNRFFVNTDMAKQKQHQKDFMTYAFGGTDR
Syn 6803        .ST.......TT......D...ER..Q.D.IKH..ADV.....RA...A.L........K
Nos com         .ST..DNI..QP.IEQV.DELHKRIATDSLLAPV.AGT..V..RN.LVA.LAQI.E.PKQ

                  fffFFFFF          gGGGGGGGGGGGGGGGGG    HHHHHHHHHHHHHHHHHHHHHH
                        7         8         9        10             11        12
                        0         0         0         0              0         0
Syn 7002        FPGRSMRAAHQDLVENAGLTDVHFDAIAENLVLTLQELNVSQD----LIDEVVTIVGSVQHRNDVLNR
Syn 6803        YD..Y..E..KE....H..NGE....V..D.LA..K.MG.PE.-----..A..AAVA.APA.KR....Q
Nos com         YG..P.DKT.AG.----N.QQP......KH.GERMAVRG..AENTKAAL.R.TNMK.AILNK
```

FIGURE 1: Amino acid sequences for *Synechococcus* sp. PCC 7002 Hb (Syn 7002), *Synechocystis* sp. PCC 6803 Hb (Syn 6803), and *Nostoc commune* GlbN (Nos com). A dot indicates a residue that is identical to that in the *Synechococcus* sp. PCC 7002 Hb sequence. The alignment was produced by BLAST (*16*). *Synechococcus* sp. PCC 7002 Hb and *Synechocystis* sp. PCC 6803 Hb have the same length and share 59% identity (positives 77%). *Synechococcus* sp. PCC 7002 Hb and *Nostoc commune* GlbN share only 29% identity (positives 50%; gaps 6%). The seven helices of the trHb fold in *C. eugametos* (*8*) are underlined with alternating solid and dashed lines and indicated with uppercase letters (A, B, C, E, F, G, and H) above the sequences. Lowercase letters indicate additional helical residues in sperm whale myoglobin (sw Mb). The histidines coordinating the iron ion in S6803 Hb (boldface, positions 46 or E10 in sw Mb and 70 or F8 in sw Mb) are conserved in the three sequences. Secondary structure assignments in the cyanobacterial proteins may be different from those in *C. eugametos* Hb. The initial Met is cleaved in the protein products.

using reversed-phase HPLC on a BetaBasic C4 column (1 × 50 mm, 3 μm packing, Keystone Scientific, Bellefonte, PA) using a model 1100 HPLC system (Hewlett-Packard, Palo Alto, CA) coupled to a Mariner mass spectrometer (Perseptive Biosystems, Framingham, MA). Gradient elution was achieved with pre-injection split and a column flow rate of approximately 50 μL/min with solvent A = 0.15% formic acid/H_2O, solvent B = 0.15% formic acid/acetonitrile, and solvent C = 0.15% formic acid/2-propanol. The solvent was programmed at A:B:C = 95:0:0 for 0−4 min, followed by a linear gradient to A:B:C = 5:95:0 at 25 min and a linear gradient to A:B:C = 5:0:95 at 40 min. All mass spectra were acquired using electrospray ionization in positive ion mode.

Optical Spectroscopy. Electronic absorption spectra were collected at 25 °C on an Aviv model 14 DS spectrophotometer and referenced to the appropriate buffer. All data were corrected for background absorption by subtracting values collected for 18 MΩ cm water over the same wavelength interval.

NMR Spectroscopy. ^{1}H NMR spectra were collected at 600 MHz on a Bruker DRX spectrometer. Samples contained the holoprotein at a concentration of ∼0.6−2 mM (per heme basis) in either 95%^1H_2O/5%^2H_2O or ^2H_2O (20 mM phosphate buffer, pH 7.5). The temperature of the samples was maintained at 25 or 35 °C. Three types of 2D experiments were performed in order to assign heme resonances: NOESY (*19*), 2QF-COSY (*20*), and clean-TOCSY (*21*, *22*). TPPI quadrature detection was applied in the indirect dimension (*23*), and the water signal was suppressed either with presaturation or with a WATERGATE sequence (*24*, *25*). Mixing times were 80 and 100 ms (NOESY) and 45 ms (TOCSY). Other spectral parameters were as described for S6803 rHb-R (*13*, *14*). In addition, WEFT data were acquired to identify rapidly relaxing protons. Post-inversion delays were varied from 5 to 120 ms in 5 ms increments, with an acquisition time and relaxation delay of 140 ms. Data were processed using either NMRPipe (*26*) or XWIN NMR (Bruker Biospin Corp., Billerica, MA).

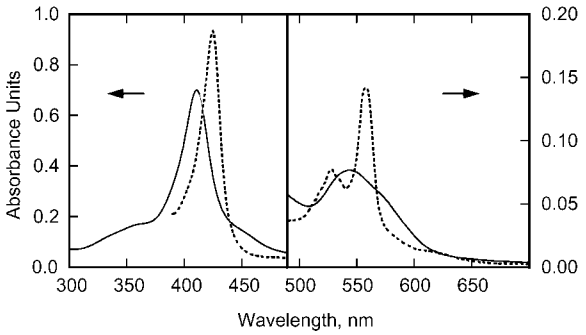

FIGURE 2: Optical absorption spectrum of S7002 rHb-R in the visible region. The protein (7 μM heme) was maintained at pH 7.5 and 25 °C. The ferric form is represented by a solid line whereas the ferrous form (reduced with dithionite) is shown as a dotted line. The arrows point to the relevant ordinates, left panel to the left and right panel to the right. Extinction coefficients and maxima are listed in Table 1.

RESULTS AND DISCUSSION

The amino acid sequence of S7002 trHb (Figure 1) is closely related to that of S6803 trHb (59% identity). Surprisingly, the next best matches (∼46% identity) are with the chloroplastic hemoglobins from *C. eugametos*, followed by the protozoan sequences from *Tetrahymena pyriformis* and *thermophila*. *N. commune* is more distantly related than these eukaryotic proteins, showing only 29% identity. These observations may indicate separate phylogenetic origins, as well as functional roles, for the trHbs found in diverse cyanobacteria.

Recombinant S7002 trHb was purified in the apoprotein form from inclusion bodies. Addition of hemin chloride yielded a stable red holoprotein, S7002 rHb-R. Mass spectrometry analysis of this species yielded a polypeptide mass of 13 726 Da (expected 13 725.6 Da); these results are consistent with the complete removal of the terminal methionine.

Optical Properties of S7002 rHb-R. Figure 2 displays the optical spectra of S7002 rHb-R obtained in the absence of

any added exogenous ligand at pH 7.5 and room temperature. The UV−visible spectrum of the ferric state showed maxima at 411 and 544 nm, and shoulders around 365, 445, and 568 nm. The absence of a charge-transfer band near 630 nm suggested an endogenous sixth ligand to the iron and low-spin electronic structure. No shoulder was observed in the 700-nm region, arguing against methionine coordination (*27*). The pyridine hemochrome spectrum of S7002 rHb-R after NMR analysis had a maximum at 557 nm and another at 525 nm, confirming that the prosthetic group was protoheme as originally inserted. The extinction coefficient of ferric S7002 rHb-R at its Soret maximum of 411 nm was determined to be 96 mM^{-1} cm^{-1}.

The spectrum of ferric S7002 rHb-R shown in Figure 2 was independent of pH down to pH ~5.4. Upon lowering the pH from 5 to 4, the intensity at 411 and 544 nm decreased while a charge-transfer band at 635 nm and a Soret at 370 nm emerged. Below pH 4, the spectrum resembled that of free heme and became independent of pH. At each pH through the transition, the observed spectrum corresponded well to a weighted sum of the two extreme spectra (neutral S7002 rHb-R and acidic free heme), suggesting the displacement of both iron axial residues and heme release upon acidification. The transition occurred over a narrow range of pH with a midpoint at pH 4.4. This pH response was in contrast to that of S6803 rHb-R, which retains a low-spin spectrum at pH 4.4 (*13*), and to that of *N. commune* GlbN, which, depending on the preparation, exhibits a mixed-spin spectrum over the range of pH 5−9 (*15*) or a transition from low to high spin below pH 6 (*5*).

Upon reduction of S7002 rHb-R by dithionite at neutral pH, the Soret peak sharpened and shifted to 425 nm, while two resolved peaks were observed at 528 nm (β) and 558 nm (α) (Figure 2), and a weak shoulder at 610 nm. The binding of carbon monoxide to the reduced protein yielded a spectrum with an absorption maximum at an intermediate value of 418 nm and at higher intensity compared to the endogenously coordinated ferric and ferrous forms; the resolved α/β peaks reverted to a single peak at 543 nm. Shoulders were detected at 397 and 513 nm, and also at 625 nm, the latter perhaps representing a contribution from free CO-bound heme. Except for the weak shoulders in the 600 nm region of the reduced states, the optical characteristics of S7002 Hb were similar to those reported for S6803 rHb-R and supported strongly the coordination of a histidine to the iron in the oxidized and reduced forms. Table 1 lists the salient features of these spectra with millimolar extinction coefficients.

NMR Assignments of the Heme and Axial Ligands of Ferric S7002 rHb-R. The one-dimensional ^1H spectrum of ferric S7002 rHb-R is shown in Figure 3A. The narrow chemical shift dispersion and sharp lines were consistent with the formation of a low-spin complex. By applying 2D homonuclear methods, the resonances from the vinyl, methyl, and propionate substituents of the porphyrin ring were identified. The heme structure and nomenclature used in this work are shown in Figure 4. The heme chemical shifts are listed in Table 2. In summary, the vinyl groups were recognized by their distinctive AMX pattern, with the α proton occurring downfield and β protons upfield from the water line. The cis and trans β protons of a given vinyl group were distinguished by using resolution-enhanced 1D data to compare the coupling constants to the α position; the proton with the larger $J_{\alpha\beta}$ value is in trans. Each of the two heme vinyl groups had NOEs to one downfield-shifted methyl group, accounting for the 2-vinyl/1-CH_3 and 4-vinyl/3-CH_3 pairs. In both cases, the β trans-to-methyl NOE was the strongest, indicating predominant vinyl orientations as drawn in Figure 4. The 1-CH_3 was identified as such by an NOE to a third heme methyl group, the 8-CH_3. The remaining heme methyl, at 24.5 ppm, was the 5-CH_3 by default. The 5- and 8-CH_3's each exhibited NOEs to a broad set of -CH_2-CH_2- resonances, attributed to the 6- and 7-propionate substituents. Figure 5 contains two sections of the TOCSY data illustrating cross-peaks for the 6-propionate candidate (*H*−*L*). The heme methyl groups occurred in the 5-1-8-3 order with a mean heme methyl shift of 14.5 ppm. The order and mean shift compared well with the data for S6803 rHb-R and indicated closely related ligation schemes and vinyl geometries (*28*).

Table 1: Optical Absorption Properties of S7002 rHb-R

Hb derivative	λ (nm)	ϵ (mM^{-1} cm^{-1})[a]
ferric	(365)	sh
	411	96
	(445)	sh
	544	10
	(568)	sh
ferrous	425	132
	528 (β)	11
	558 (α)	21
ferrous + CO	(397)	sh
	418	165
	(513)	sh
	543	13

[a] Spectra are shown in Figure 2. Values were determined by the hemochromogen method (*18*) with samples of the ferric protein; values in parentheses and marked "sh" denote a shoulder to the main peak. Additional shoulders are discussed in the text.

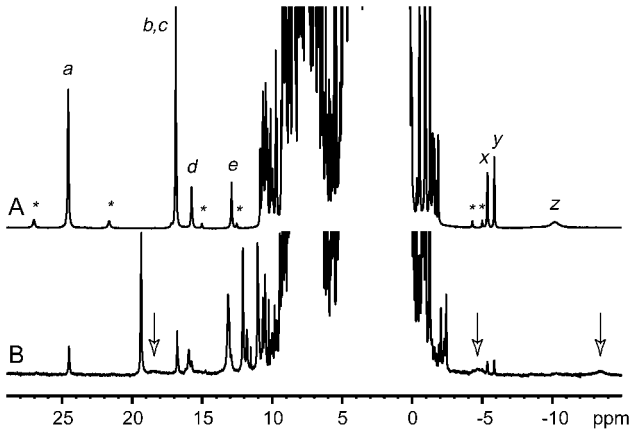

FIGURE 3: 600 MHz ^1H NMR spectrum of recombinant S7002 Hb-R in the ferric state. (A) The protein (2 mM heme) was in 95% H_2O/5% ^2H_2O, buffered at pH 7.5 with 20 mM sodium phosphate; the probe temperature was 25 °C. The letters indicate hyperfine-shifted signals (Tables 2 and 3). Peaks *d* and *e* arise from labile protons and are not observed in ^2H_2O solutions. The asterisks indicate a minor protein form integrating as 8% of the total sample. This form is attributed to heme rotational isomerism. (B) Spectrum of a mixture containing the form shown in (A) as well as a species that does not release the heme upon acid−butanone extraction. This latter species accounts for 80% of this particular sample. Arrows point to broad peaks consistent with the CδH and CϵH of axial histidines in this second form.

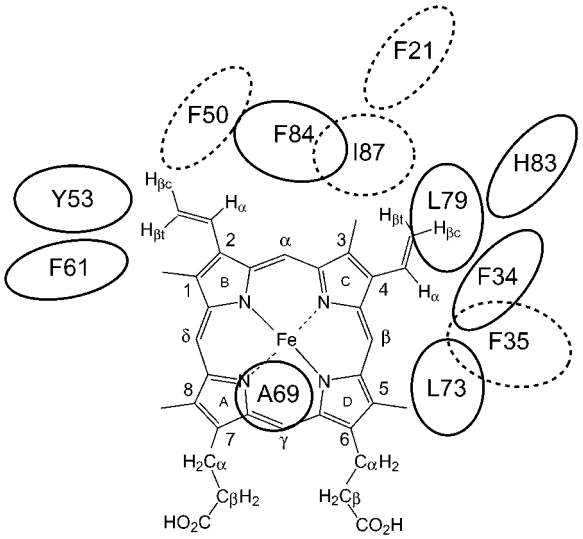

FIGURE 4: Structure of iron-protoporphyrin IX and the nomenclature used in this work. The residues mentioned in the text are positioned around the periphery of the heme, using the primary structure of S7002 Hb. Dashed lines indicate residues on the distal side of the heme; continuous lines, residues on the proximal side according to a preliminary solution structure of S6803 Hb and the properties of the trHb fold (*8*). In S6803 Hb, Phe61 is replaced with Tyr61, and Ile87 with Val87.

Table 2: ^{1}H NMR Chemical Shifts for Heme Resonances in the Spectrum of Ferric S7002 rHb-R

assignment	signal[a]	δ (ppm)[b]	assignment	signal[a]	δ (ppm)[b]
5-methyl	a	24.54	7-α′-propionate		1.41
1-methyl	b	16.86	6-*β*-propionate		1.24
2-α-vinyl	c	16.81	6-*β*′-propionate		0.50
6-α-propionate		10.40	7-*β*-propionate		−1.01
6-α′-propionate		9.95	7-*β*′-propionate		−1.50
8-methyl		9.22	*trans*-4-*β*-vinyl		−1.60
3-methyl		7.16	*cis*-4-*β*-vinyl		−1.90
4-α-vinyl		5.20	*trans*-2-*β*-vinyl	x	−5.41
7-α-propionate		2.12	*cis*-2-*β*-vinyl	y	−5.91

[a] Refer to Figure 3A for peak labeling and to Figure 4 for the heme structure. [b] In 95% ^1H_2O/5% ^2H_2O, at 25 °C and pH 7.6, with the water resonance set at 4.76 ppm with respect to DSS.

Returning to Figure 3A, peak *z* at −10.4 ppm has chemical shift and line width typical of an axial imidazole C*δ*H or C*ϵ*H (*28*), and supports the coordination of one histidine to the iron. The WEFT data shown in Figure 6 revealed three other protons with relaxation properties similar to those of peak *z*. Table 3 contains the chemical shifts for these peaks as well as those for similar resonances observed in WEFT data of S6803 rHb-R (*14*). The presence of these four signals was consistent with the ligation of two histidines through their N*ϵ* atom. Additional evidence was provided by peaks *d* and *e* (Figure 3A), which disappeared in ^2H_2O. In S6803 rHb-R, they arise from the N*δ*H of the axial histidines (*14*). Figure 7 contains S7002 rHb-R NOESY data that established connectivity between *d* and 10.71 ppm, and *e* and 10.44 ppm. These 10−11 ppm signals belong to AMX spin systems (*A*−*C* and *D*−*F*, Figure 5), consistent with -C*β*H$_2$-CαH- moieties. The correlated data in ^1H_2O extended these to include the corresponding peptide NHs. The chemical shifts for the C*β*H$_2$-CαH-NH units are listed in Table 3. S7002 Hb contains a total of four histidines; TOCSY data collected in ^2H_2O solutions showed two sets

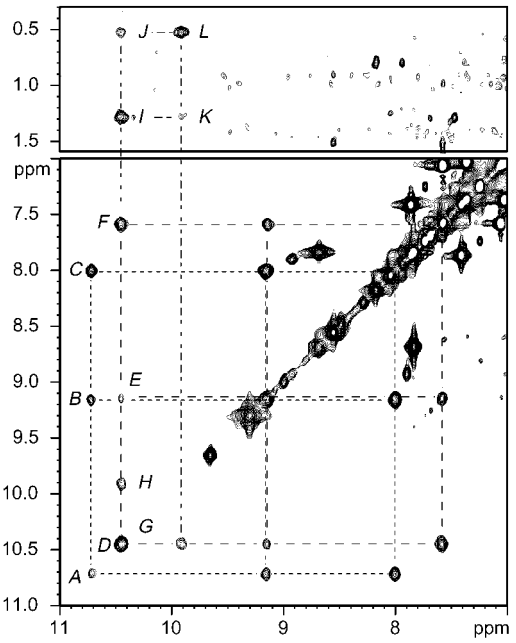

FIGURE 5: Portion of the ^{1}H-^{1}H clean TOCSY data for recombinant S7002 Hb-R in the ferric state. Data were collected at 600 MHz at a protein concentration of 1.5 mM on a per-heme basis. The solvent was ^2H_2O, buffered at pH 7.5 (uncorrected for isotope effects) with 20 mM sodium phosphate; the probe temperature was 25 °C. The mixing time was 45 ms. Squared-cosine bells were applied in both dimensions prior to Fourier transformation in order to preserve the broad peaks in this region. The labels indicate: His46 C*β*H (*A*), His46 C*β*H to His46 C*β*H′ (*B*), His46 C*β*H to His46 CαH (*C*), His70 C*β*H (*D*), His70 C*β*H to His70 C*β*H′ (*E*), His70 C*β*H to His70 CαH (*F*), 6-α-propionate (*G*), 6-α-propionate to 6-α′-propionate (*H*), 6-α-propionate to 6-*β*-propionate (*I*), 6-α-propionate to 6-*β*′-propionate (*J*), 6-α′-propionate to 6-*β*-propionate (*K*), and 6-*β*′-propionate (*L*). In the 2QF-COSY data, cross-peaks *J* and *K* are intense, and cross-peaks *I* and *L* are weak. Chemical shifts are listed in Tables 2 and 3.

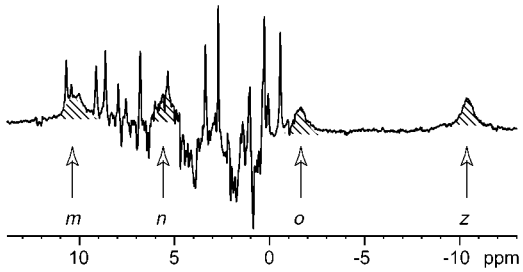

FIGURE 6: WEFT NMR spectrum of ferric S7002 rHb-R. Data were collected at 600 MHz and 25 °C on the same sample as in Figure 5. The trace is a difference between two spectra: one with a WEFT recovery delay of 15 ms, the other with a recovery of 5 ms. This emphasizes resonances with the shortest T_1 value. The time-domain data were subjected to a line-broadening of 20 Hz prior to transformation. Four broad resonances are observed (hatched) and marked by arrows: *m* (10.2 ppm), *n* (5.4 ppm), *o* (−1.7 ppm), and *z* (−10.4 ppm); these signals are tentatively assigned to the C*δ*H and C*ϵ*H of the axial histidines.

of resolved and sharp cross-peaks corresponding to the C*δ*H-C*ϵ*H connectivities of two rings, as expected if the other two imidazoles were involved in the complex and yielded peaks *m*, *n*, *o*, and *z* (Figure 6). S7002 Hb also contains seven phenylalanines and three tyrosines. All these aromatic rings could be accounted for in the 9-to-5 ppm region of the 2QF-COSY data, a portion of which is shown in Figure 8. The ensemble of the NMR data was therefore in

Table 3: ^{1}H NMR Chemical Shifts for the Axial Histidines in the Spectrum of Ferric S7002 rHb-R

assignment	signal[a]	δ (ppm)[b] S7002	δ (ppm)[c] S6803
His46 NH		10.65	10.67
His46 CαH		7.97	7.70
His46 CβH		10.71	10.82
His46 CβH		9.15	9.20
His46 NδH	e	12.88	13.2
His70 NH		10.40	9.90
His70 CαH		7.57	6.75
His70 CβH		10.44	9.72
His70 CβH		9.14	8.92
His70 NδH	d	15.73	15.0
−	m	10.2[d]	11.7[e]
−	n	5.4[d]	5.4[e]
−	o	−1.7[d]	−1.7[e]
−	z	−10.4[d]	−10.8[e,f]

[a] Refer to Figure 3A for peak labeling. [b] In 95% ^1H_2O/5% ^2H_2O, at 25 °C and pH 7.6, with the water resonance set at 4.76 ppm with respect to DSS (this work). [c] Measured in 95% H_2O/5% ^2H_2O, pH 6.9−7.5, 25 °C (*14*). [d] In ^2H_2O, pH 7.6, 25 °C (this work); refer to Figure 6 for peak labeling. [e] In ^2H_2O, pH 7.2, 35 °C (*14*). [f] Assigned to His46 CϵH (*14*).

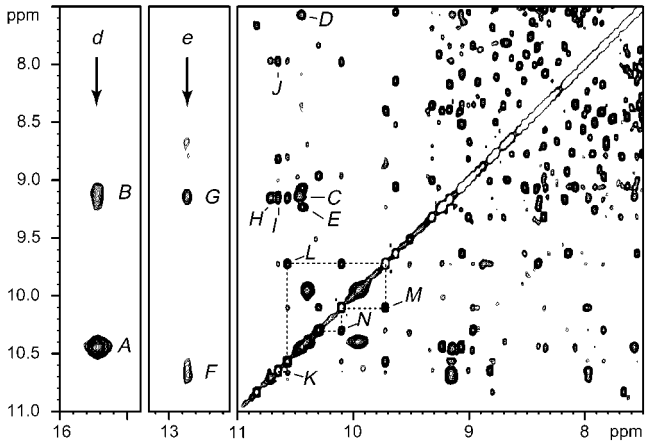

FIGURE 7: Portions of the ^{1}H NOESY data for recombinant S7002 Hb-R in the ferric state. Spectra were acquired at 600 MHz and 25 °C on the same sample as in Figure 3. The left two panels are from a spectrum collected with presaturation of the water line, and the right panel is from a spectrum collected with WATERGATE solvent suppression. Cross-peaks are as follows, with identity in the direct dimension given first: His70 NδH (signal *d* in Figure 3A) to His70 CβH (*A*) and His70 CβH′ (*B*); His70 CβH to His70 CβH′ (*C*); His70 NH to His70 CαH (*D*) and Ala69 NH (*E*); His46 NδH to His46 CβH (*F*) and His46 CβH′ (*G*); His46 CβH to His46 CβH′ (*H*); His46 NH to His46 CβH (*I*) and His46 CαH (*J*); Gln47 NH to His46 NH (*K*) and Lys48 NH (*L*); Lys48 NH to Asp49 NH (*M*); and Asp49 NH to Phe50 NH (*N*). Chemical shifts are listed in Tables 2 and 3, and in the Supporting Information. The rest of the right panel illustrates a large number of NH−NH connectivities as expected of a helical protein.

agreement with coordination of the heme by His46 and His70.

Heme Environment in S6803 rHb-R and S7002 rHb-R. In low-spin ferric heme proteins, the chemical shifts of the axial histidine protons are highly dependent on the orientation of the imidazole rings with respect to the heme group. Thus, additional analyses of the spectra were necessary to assign the shifted CβH_2-CαH-NH units to His46 or His70. In S6803 rHb-R, for which the ^{1}H, ^{13}C, and ^{15}N assignments are practically complete (*29*), several aromatic and aliphatic side chains were found in dipolar contact with the prosthetic

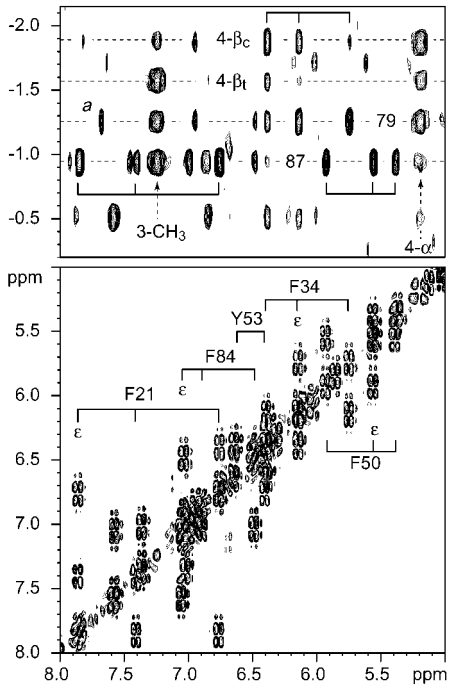

FIGURE 8: Portions of the ^{1}H-^{1}H NOESY data and 2QF-COSY data for recombinant S7002 Hb-R in the ferric state. Spectra were at 600 MHz and 25 °C on the same sample as in Figure 5. The bottom panel shows the aromatic region of the 2QF-COSY spectrum. The top panel contains the NOEs to the 4-β vinyl and two upfield-shifted residues identified as Ile87 (CδH_3 overlapping with CγH_3 under these conditions) and Leu79 (CδH_3). Note the effects to the aromatic residues: 4-β-vinyl to Phe34, Leu79 to Phe34 and His83 (labeled *a*), Ile87 to Phe50 and Phe21. These effects are shown in Figure 9 for S6803 rHb-R.

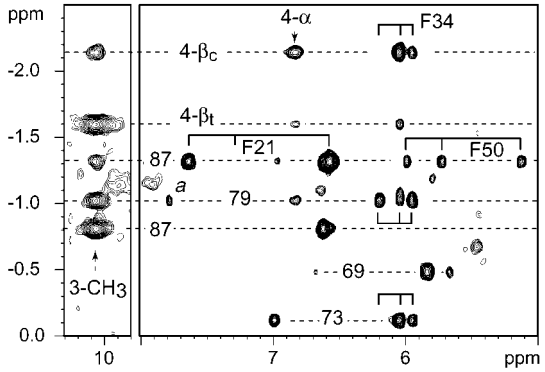

FIGURE 9: Portions of the ^{1}H NOESY data for recombinant S6803 Hb-R in the ferric state. Spectra were at 600 MHz at a protein concentration of 1 mM on a per-heme basis in ^2H_2O, buffered at pH 7.2 with 20 mM sodium phosphate; the probe temperature was 25 °C. The locations of the ring signals for Phe21, Phe34, and Phe50 are indicated. The labels 87, 79, 69, and 73 indicate the location of methyl groups: Val87 CγH_3's, Leu79 CδH_3, Ala69 CβH_3, and Leu73 CδH_3, respectively. The label *a* denotes an NOE between Leu79 and His83 CϵH.

group. To illustrate a few residues relevant to this study, Figure 9 presents NOEs from pyrrole C to Leu79, Val87, and Phe34. Phe34 in turn had NOEs to both Leu79 and Leu73. Leu79 was near His83 and Leu73; and Leu73 displayed NOEs to the heme 5-CH_3 (not shown). Val87 was in contact with Phe50, a residue showing strong NOEs to the 2-vinyl group (pyrrole B), and with Phe21, a residue further from the heme and on its distal side. Not shown are interactions between the 2-vinyl substituent and Tyr53 and

Phe84; interactions between Tyr61 and the heme 1-CH_3; and interactions between Phe35 and the heme 5-CH_3. These residues (or their S7002 Hb counterparts) are outlined in Figure 4 at their approximate location relative to the heme group.

A comparable network of dipolar contacts was detected in S7002 rHb-R, some of which are shown in the NOESY panel of Figure 8. For example, the 4-vinyl group had distinctive NOEs to a phenylalanine ring also in contact with a leucine side chain near the 3-CH_3. This accounted for Phe34 and Leu79. Leu79 showed NOEs to another leucine near the heme 5-CH_3 (not shown), corresponding to Leu73, and to one of the two noncoordinating histidines (His83). The 3-CH_3 had strong NOEs to an upfield-shifted isoleucine spin system in contact with a phenylalanine ring, itself near the 2-vinyl group. This was in agreement with the Ile87/Phe50 pair. Ile87 had NOEs to an additional phenylalanine ring, not in contact with the heme, and corresponding to Phe21. NOEs were also obtained from the 2-vinyl substituent to a tyrosine ring (Tyr53) and a phenylalanine ring (Phe84); the heme 1-CH_3 was found close to yet another phenylalanine (Phe61). The chemical shifts of these residues are listed in the Supporting Information. The partial survey of the heme periphery revealed that the chemical shift of the residues common to the two proteins, although understandably not identical, followed similar trends compared to random values. The NOEs observed in S7002 rHb-R also argued for the same prosthetic group orientation within the protein matrix as in S6803 rHb-R. The preference for this orientation is greater than 90% in both proteins.

With the assignments proposed above and the pronounced parallel between the two proteins, the axial histidine signals were considered further. The peptide NH at 10.65 ppm had resolved dipolar connectivities characteristic of α-helical structure (Figure 7). By following these effects and analyzing the *J*-correlated data belonging to the sequential NH's, a pattern consistent with the polypeptide chain beyond His46 could be traced. As expected, at position $i + 4$ from His46 was found a peptide NH with an NOE to the ring assigned above as Phe50. The sequence of NH chemical shifts in this region of the protein resembled that observed for S6803 rHb-R. Likewise, the residue prior to the peptide NH at 10.40 ppm was identified as an alanine (*J*-correlated data and NOEs between the β-CH_3 and the peptide NH), consistent with the Ala69-His70 sequence. The same effects were observed in S6803 Hb, although in this protein the β-CH_3 of Ala69 is under the influence of the Tyr65 ring, as opposed to Ser65 in S7002 Hb, and is shifted upfield (Figure 9). Finally, Leu73 had NOEs to the C$\beta$$H_2$-C$\alpha$H portion of His70. Assignments obtained in this fashion represent a self-consistent initial set; they will be confirmed and expanded beyond the heme environment with isotopically labeled protein.

The steric constraints imposed by ligation of His46 and His70 limit the number of conformational possibilities for the polypeptide chain in the E−F region, and it is therefore not surprising to observe similar geometries and shifts for many side chains in the two rHb-R's. From the spectroscopic viewpoint, it is noteworthy that the chemical shifts of His46 match well in the two proteins, whereas those of the proximal histidine are systematically displaced downfield on average by −0.6 ppm in S7002 rHb-R. This observation has bearing on the electronic structure of the heme group and will be useful when correlating paramagnetic properties and structural details.

Stability of S7002 rHb-R and Formation of a Covalent Heme Adduct. The spectral analysis presented above pertains to signals from S7002 rHb-R in the ferric state. After several days at conditions suitable for NMR studies (as in Figure 3A), some of the S7002 rHb-R samples underwent a remarkable transformation by which the spectrum changed gradually from the trace in Figure 3A to that in Figure 3B. In Figure 3B, rHb-R is still recognizable, but most of the protein has converted to a new species, henceforth S7002 rHb-A. The chemical shift dispersion observed for S7002 rHb-A and the presence of broad and shifted peaks typical of axial histidine CδH and CϵH suggested strongly that the coordination scheme of rHb-R was maintained. In contrast to S7002 rHb-R, S7002 rHb-A did not lose the heme group when subjected to the acid−butanone extraction protocol of Teale (*30*). Additionally, mass spectroscopic data returned a molecular weight for S7002 rHb-A that equaled within experimental error the sum of the masses of the apoprotein and free heme. Survival of the heme−protein couple through these two treatments was evidence that the conversion involved the formation of a covalent linkage between the protein and its prosthetic group.

Minor changes in the electronic absorption spectrum were observed on going from S7002 rHb-R to rHb-A. The Soret maximum moved to 409 nm with the blue shoulder at about 360 nm, while the secondary peak was slightly red-shifted at 545 nm. These small perturbations made optical detection of ferric S7002 rHb-A in a sample of S7002 rHb-R difficult. The pyridine−hemochromogen assay of the holoprotein rendered by the Teale procedure (S7002 rHb-A) exhibited maxima at 552 and 522 nm, values within 1−2 nm of the maxima characteristic of hematoheme [551 and 520 nm, (*31*)] and *c*-type cytochromes [550 and ∼521 nm, (*32*)]; this supported a modification of a heme vinyl group, a probable candidate for the attachment site to the polypeptide. Conversion of rHb-R to species containing a modified heme was previously observed with S6803 rHb-R (*14*). In this case, hemochrome analysis appeared to return a normal iron-protoporphyrin IX spectrum. Reinspection of the properties of S6803 rHb-A on samples that converted completely yielded a hematoheme-like spectrum as for S7002 rHb-A.

Preliminary NMR data were collected on S7002 rHb-A in order to examine the modified heme signals. Figure 10A shows the 20-to-4 ppm region of a sample containing approximately 90% rHb-A at 35 °C. Resonances *m1*, *m2*, *m3*, and *m4* had the intensity, shift, and width expected of the four methyl groups of low-spin iron-protoporphyrin IX. In the clean-TOCSY experiment, signals *v1* and *v2* were correlated to a signal at 6.89 ppm, with *v1* exhibiting a larger coupling constant than *v2* (Figure 10B,C). In addition, *v1* and *v2* had medium and weak NOEs, respectively, to *m3* (Figure 10D,E). No NOE was detected between *m3* and any of the other heme methyl groups, whereas a small effect was observed between *m2* and *m4* (Figure 10F,G). Signal *m1* also lacked inter-methyl effects. The simplest interpretation of the data assigned *m3* as the 3-CH_3 and the *v1*-*v2*-6.95 ppm AMX system to the intact 4-vinyl group. Although the vinyl groups of iron-protoporphyrin IX are readily detected in rHb-R and other *b* hemoproteins, the rHb-A data contained

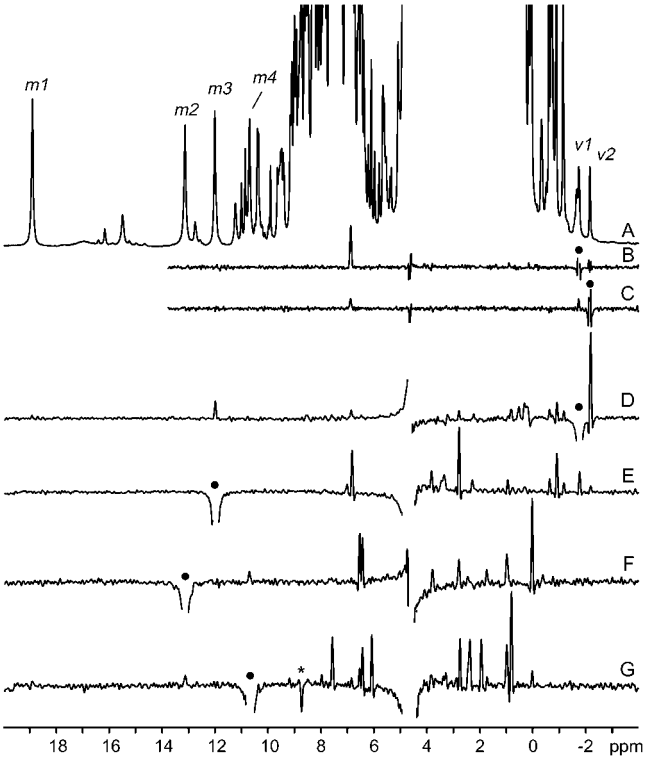

FIGURE 10: Rows of the clean-TOCSY and NOESY data for S7002 rHb-A. Spectra were acquired at 600 MHz at a protein concentration of 0.6 mM on a per-heme basis. The solvent was 95% ^1H_2O/5% ^2H_2O, buffered at pH 6.8 with 20 mM sodium phosphate; the probe temperature was 35 °C. The spectra were referenced through water at 4.65 ppm. In traces B−G, the filled circle indicates the diagonal peak (in D−G, only resolution enhancement wings are shown). A star in G indicates an artifact. (A) Reference 1D spectrum between 20 and −4 ppm. The complete spectrum at 25 °C is shown in Figure 3B. (B,C) TOCSY connectivities between *v1* and 6.89 ppm (B) and between *v2* and 6.89 ppm (C). The data were collected with a 45 ms mixing time and WATERGATE suppression of the water. The spectral width in the direct dimension was 11 kHz. A squared-sine bell was applied in the direct (45°) and indirect (90°) dimensions prior to transformation. (D−G) NOESY connectivities for *v1* (D), *m3* (E), *m2* (F), and *m4* (G). The data were collected with a 100 ms mixing time and presaturation of the water line. The spectral width in the direct dimension was 18.4 kHz. A squared-sine bell was applied in the direct (45°) and indirect (90°) dimensions prior to transformation. In (D), note the effect between *v1* and *m3*; this effect is also seen in (E). In (F) and (G), a weak but reproducible NOE is observed between *m2* and *m4*; these two methyls also have a number of NOEs in common, in support of assignment to CH_3's on pyrroles A and B. Inspection of the effects from *m2* and *m4* does not reveal a candidate vinyl group. The data are consistent with assignment of *m1* to the heme 5-CH_3 (trace not shown).

no obvious spin system attributable to a second vinyl in contact with either *m2* or *m4*. Thus, the cross-link responsible for the hemochromogen result occurred through the 2-vinyl side chain. During initial experiments to localize the point of attachment on the protein, it was observed that rHb-A was resistant to tryptic digestion under conditions that easily fragmented rHb-R.

The ability of the heme pocket to select for a specific orientation of the heme group may have special significance as it positions the same vinyl groups in proximity to the same protein residues in the majority of the holoprotein molecules. Furthermore, this nearly uniform orientation is common to both S6803 rHb and S7002 rHb, whereas the GlbN protein from *N. commune* favors the reverse by 80% (*33*). It remains to be determined whether the chemical modification observed with recombinant material in vitro takes place in the cyanobacterial cells. Nevertheless, the ease with which the conversion takes place suggests adduct formation should be taken into account when proceeding with biochemical analyses. Autocatalytic formation of a cross-link between heme and protein has been reported for various peroxidases (*34*, *35*) and recently in cytochrome P4504A fatty acid hydroxylase (*36*). In lactoperoxidase (*34*, *37*, *38*), the cross-links result from heme methyl reaction with carboxylic acids to form esters. In rHb-A, the heme methyl groups appeared intact. The nature of the cross-link and the chemistry underlying its formation are currently under investigation.

SUMMARY

Endogenous, reversible hexacoordination is atypical of hemoglobins but is found in an increasing number of vertebrate and invertebrate examples. These include human and mouse neuroglobins (*39*, *40*), *C. eugametos* chloroplastic Hb (*41*), and the nonsymbiotic hemoglobin from rice, for which it is thought to play a role in controlling ligand affinity (*42*). Coordination of a protein side chain to the distal position of the iron is expected to influence both the dynamic and structural features of the hemoglobin. It is clear that axial ligand strength is an essential property of the molecule that must be considered in order to rationalize the kinetics of ligand binding as well as alternative functional roles.

The ferric hemoglobin from *Synechococcus* sp. PCC 7002 shares several physical properties with its relative from *Synechocystis* sp. PCC 6803. S7002 rHb readily forms a hexacoordinate, low-spin complex in the absence of exogenous ligand. Only two forms of the protein were necessary to explain the appearance of the NMR spectra of rHb-R: one in which the heme is oriented as in the major form of S6803 rHb-R and one in which the heme was rotated by 180° about the $\alpha-\gamma$ meso axis. Interestingly, there was no detectable amount of alternative coordination schemes (pentacoordinate, or a different ligand) in the ferric state over a range of pH values. All spectral manifestations (optical and magnetic resonance) supported a bis-histidine ligation to the heme involving His46 (E10) as the ligand on the distal side. The heme pocket, lined with several aromatic residues, was capable of discriminating the substituents at the 1, 2, 3, and 4 positions of the heme ring. The ready formation of a derivative species in which the heme is covalently bound to the protein through a vinyl group showed that the Hbs of both S7002 and S6803 are capable of similar chemistry. The biochemical and structural similarities of these proteins suggest that they play similar roles in cellular physiology and metabolism.

ACKNOWLEDGMENT

We thank Dr. Jürgen Marquardt for providing the cosmid and the sequence data, B. Christie Vu for assistance with the S6803 aspects of the project, and Dr. A. D. Jones for the collection of mass spectrometry data. The mass spectrometer (Penn State Intercollegiate Center for Mass Spectrometry) and the Bruker DRX-600 NMR spectrometer were purchased in part with funds from the National Institutes of

Health, Grant S10 RR11318 and Grant S10 RR10524, respectively.

SUPPORTING INFORMATION AVAILABLE

Table listing the chemical shifts for the residues discussed in the text. The chemical shifts of S6803 rHb-R are available from the BioMagResBank (http://www.bmrb.wisc.edu) under accession number BMRB-5269. This information is available free of charge via the Internet at http://pubs.acs.org.

REFERENCES

1. Potts, M., Angeloni, S. V., Ebel, R. E., and Bassam, D. (1992) *Science 256*, 1690−1691.
2. Kaneko, T., Sato, S., Kotani, H., Tanaka, A., Asamizu, E., Nakamura, Y., Miyajima, N., Hirosawa, M., Sugiura, M., Sasamoto, S., Kimura, T., Hosouchi, T., Matsuno, A., Muraki, A., Nakazaki, N., Naruo, K., Okumura, S., Shimpo, S., Takeuchi, C., Wada, T., Watanabe, A., Yamada, M., Yasuda, M., and Tabata, S. (1996) *DNA Res. 3*, 109−136.
3. Hill, D. R., Belbin, T. J., Thorsteinsson, M. V., Bassam, D., Brass, S., Ernst, A., Boger, P., Paerl, H., Mulligan, M. E., and Potts, M. (1996) *J. Bacteriol. 178*, 6587−6598.
4. Wittenberg, J. B., Bolognesi, M., Wittenberg, B. A., and Guertin, M. (2002) *J. Biol. Chem. 277*, 871−874.
5. Thorsteinsson, M. V., Bevan, D. R., Ebel, R. E., Weber, R. E., and Potts, M. (1996) *Biochim. Biophys. Acta 1292*, 133−139.
6. Kaneko, T., Nakamura, Y., Wolk, C. P., Kuritz, T., Sasamoto, S., Watanabe, A., Iriguchi, M., Ishikawa, A., Kawashima, K., Kimura, T., Kishida, Y., Kohara, M., Matsumoto, M., Matsuno, A., Muraki, A., Nakazaki, N., Shimpo, S., Sugimoto, M., Takazawa, M., Yamada, M., Yasuda, M., and Tabata, S. (2001) *DNA Res. 8*, 205−213.
7. DOE Joint Genome Institute: http://spider.jgi-psf.org/JGI_microbial/html/.
8. Pesce, A., Couture, M., Dewilde, S., Guertin, M., Yamauchi, K., Ascenzi, P., Moens, L., and Bolognesi, M. (2000) *EMBO J. 19*, 2424−2434.
9. Milani, M., Pesce, A., Ouellet, Y., Ascenzi, P., Guertin, M., and Bolognesi, M. (2001) *EMBO J. 20*, 3902−3909.
10. Das, T. K., Weber, R. E., Dewilde, S., Wittenberg, J. B., Wittenberg, B. A., Yamauchi, K., Van Hauwaert, M. L., Moens, L., and Rousseau, D. L. (2000) *Biochemistry 39*, 14330−14340.
11. Couture, M., Das, T. K., Savard, P. Y., Ouellet, Y., Wittenberg, J. B., Wittenberg, B. A., Rousseau, D. L., and Guertin, M. (2000) *Eur. J. Biochem. 267*, 4770−4780.
12. Hvitved, A. N., Trent, J. T., III, Premer, S. A., and Hargrove, M. S. (2001) *J. Biol. Chem. 276*, 34714−34721.
13. Scott, N. L., and Lecomte, J. T. J. (2000) *Protein Sci. 9*, 587−597.
14. Lecomte, J. T. J., Scott, N. L., Vu, B. C., and Falzone, C. J. (2001) *Biochemistry 40*, 6541−6552.
15. Thorsteinsson, M. V., Bevan, D. R., Potts, M., Dou, Y., Eich, R. F., Hargrove, M. S., Gibson, Q. H., and Olson, J. S. (1999) *Biochemistry 38*, 2117−2126.
16. Altschul, S. F., Madden, T. L., Schäffer, A. A., Zhang, J., Zhang, Z., Miller, W., and Lipman, D. J. (1997) *Nucleic Acids Res. 25*, 3389−3402.
17. Hanahan, D. (1985) in *DNA Cloning, A Practical Approach* (Glover, D. M., Ed.) pp 109−135, IRL Press, Washington, DC.
18. de Duve, C. (1948) *Acta Chem. Scand. 2*, 264−289.
19. Kumar, A., Ernst, R. R., and Wüthrich, K. (1980) *Biochem. Biophys. Res. Commun. 95*, 1−6.
20. Rance, M., Sørensen, O. W., Bodenhausen, G., Wagner, G., Ernst, R. R., and Wüthrich, K. (1983) *Biochem. Biophys. Res. Commun. 117*, 479−485.
21. Braunschweiler, L., and Ernst, R. R. (1983) *J. Magn. Reson. 53*, 521−528.
22. Cavanagh, J., and Rance, M. (1992) *J. Magn. Reson. 96*, 670−678.
23. Drobny, G., Pines, A., Sinton, S., Weitekamp, D. P., and Wemmer, D. (1979) *Symp. Faraday Soc. 13*, 49−55.
24. Sklenár, V., Piotto, M., Lepik, R., and Saudek, V. (1993) *J. Magn. Reson. 102*, 241−245.
25. Piotto, M., Saudek, V., and Sklenár, V. (1992) *J. Biomol. NMR 2*, 661−665.
26. Delaglio, F., Grzesiek, S., Vuister, G. W., Zhu, G., Pfeifer, J., and Bax, A. (1995) *J. Biomol. NMR 6*, 277−293.
27. Dickerson, R. E., and Timkovich, R. (1975) in *The Enzymes* (Boyer, P., Ed.) pp 397−492, Academic Press, New York.
28. La Mar, G. N., Satterlee, J. D., and de Ropp, J. S. (2000) in *The Porphyrins Handbook* (Smith, K. M., Kadish, K., and Guilard, R., Eds.) pp 185−298, Academic Press, Burlington, MA.
29. Falzone, C. J., and Lecomte, J. T. J. (2002) *J. Biomol. NMR* (in press).
30. Teale, F. W. J. (1959) *Biochim. Biophys. Acta 35*, 543.
31. Antonini, E., and Brunori, M. (1971) *Hemoglobin and myoglobin in their reactions with ligands*, Vol. 12, North-Holland, Amsterdam.
32. Berry, E. A., and Trumpower, B. L. (1987) *Anal. Biochem. 161*, 1−15.
33. Yeh, D. C., Thorsteinsson, M. V., Bevan, D. R., Potts, M., and La Mar, G. N. (2000) *Biochemistry 39*, 1389−1399.
34. DePillis, G. D., Ozaki, S., Kuo, J. M., Maltby, D. A., and Ortiz de Montellano, P. R. (1997) *J. Biol. Chem. 272*, 8857−8860.
35. Oxvig, C., Thomsen, A. R., Overgaard, M. T., Sørensen, E. S., Højrup, P., Bjerrum, M. J., Gleich, G. J., and Sottrup-Jensen, L. (1999) *J. Biol. Chem. 274*, 16953−16958.
36. Hoch, U., and Ortiz De Montellano, P. R. (2001) *J. Biol. Chem. 276*, 11339−11346.
37. Rae, T. D., and Goff, H. M. (1996) *J. Am. Chem. Soc. 118*, 2103−2104.
38. Rae, T. D., and Goff, H. M. (1998) *J. Biol. Chem. 273*, 27968−27977.
39. Burmester, T., Weich, B., Reinhardt, S., and Hankeln, T. (2000) *Nature 407*, 520−523.
40. Trent, J. T., III, Watts, R. A., and Hargrove, M. S. (2001) *J. Biol. Chem. 276*, 30106−30110.
41. Das, T. K., Couture, M., Lee, H. C., Peisach, J., Rousseau, D. L., Wittenberg, B. A., Wittenberg, J. B., and Guertin, M. (1999) *Biochemistry 38*, 15360−15368.
42. Hargrove, M. S., Brucker, E. A., Stec, B., Sarath, G., Arredondo-Peter, R., Klucas, R. V., Olson, J. S., and Phillips, G. N. (2000) *Struct. Fold. Des. 8*, 1005−1014.

BI025609M